Photosynthesis Research **47**: 61–76, 1996.

Regular paper

Improved 5-step modeling of the Photosystem II S-state mechanism in cyanobacteria

Pascal C. Meunier[1], Robert L. Burnap[2] & Louis A. Sherman[1]
[1]*Department of Biological Sciences, Purdue University, West Lafayette, IN 47907, USA;* [2]*Department of Microbiology and Molecular Genetics, Oklahoma State University, Stillwater, OK 74078, USA*

Received 24 July 1995; accepted in revised form 1 November 1995

Key words: Cyanothece sp. ATCC 51142, *psbO* deletion mutant, *Synechocystis* sp. PCC 6803, S_{-1}

Abstract

We present a model of the S-state mechanism, as well as an improved eigenvalue analysis, that integrate into a coherent ensemble several features found since the S-state model was initially developed. These features include the presence of S_{-1}, deactivations in the dark interval between flashes, and the change in the number of active PS II centers by photoinhibition or photoactivation. A new feature is the capacity to predict the steady-state distribution of S-states under conditions of steady photoinhibition or photoactivation. The improved eigenvalue analysis allowed the calculation of the initial S-state distribution. In addition, the model resolved 'true' photochemical misses from apparent misses due to deactivations in the dark interval between flashes. The model suggested that most of the misses that are commonly reported are due to deactivations, and not to an intrinsic inefficiency of the photochemical mechanism of PS II. Because models that allow double-hits encompassing the S_2 to S_3 transition often predict negative initial quantities of S_2 in cyanobacteria, our proposed model specifically prohibited them. The model accounts for inhomogeneous misses and a steady-state distribution of the type $(S_2)\approx(S_1)>(S_3)\approx(S_0)$. This 5-step model uses only 4 probabilities, and is therefore easy to handle. The use of this model is critical for the analysis of several cyanobacterial strains, as well as for any species that show non-negligible deactivations in the dark interval between flashes.

Introduction

Oxygen production under short light flashes results in yields of oscillating amplitudes (Joliot et al. 1969). The oxygen production mechanism was modeled as a 4-step mechanism, S_0 to S_3, in addition to a non-observable, transient S_4 (Kok et al. 1970). Transitions between the 4 (indirectly) observable states S_0 to S_3 were modeled with homogeneous miss, single-hit and double-hit probabilities (Forbush et al. 1971). However, the knowledge of the properties of the S-state mechanism has increased since then. It was found that an S_{-1} state, and sometimes an S_{-2} state, were necessary to describe the O_2 production sequences (Thibault 1982; Bader et al. 1983; Messinger and Renger 1993). It has been suggested that the transition probabilities between S-states were most likely inhomogeneous (Delrieu 1974; Lavorel 1976; Delrieu 1983). The interaction of the oxidizing side of PS II with the tyrosine 'D' was also discovered to distort the extrapolated initial distribution of S-states and to increase misses (Vermaas et al. 1984; Styring and Rutherford 1987). The role of the plastoquinone pool in controlling misses through deactivations was investigated, and a distinction was made between 'true' misses and single-hits followed by deactivations (Meunier and Popovic 1990). The anomalous behavior of double-hits was noted (Delrieu 1983), and a probability for backward transitions was added (Meunier 1993). In addition, the number of PS II centers contributing to the oxygen yields was found to decrease at each flash (Delrieu and Rosengard 1987) or increase with the photoactivation of new centers, yielding a sum of probabilities different from 100% (Meunier and Popovic 1990; Meunier

and Popovic 1991). However, when faced with experimental data, there is no reliable (yet not too complex) model that allows for the integration of those features, with the capacity to calculate the initial and the steady-state distributions of S-states. In addition, we found that none of the published models could satisfactorily explain the oxygen yields obtained in certain cyanobacterial strains, especially the *psbO*-less mutant of *Synechocystis* sp. PCC 6803 (Burnap and Sherman 1991) and *Cyanothece* sp. ATCC 51142 (Meunier and Sherman, unpublished observations), which both show reversible inactivation and reactivation of manganese in Photosystem II.

It remains difficult to extract practical and meaningful information in a timely manner from the oxygen yield sequences. At the root of the problem is the fact that for an N-step mechanism, there are only 2N variables that can be determined from the O_2 yield sequence: N for the transition probabilities (the transition matrix) and N for the initial S-state distribution. By contrast, there are at least $N+N^2$ unknowns: N for the initial distribution of S-states, and N^2 for the probabilities in the $N \times N$ matrix (considering only the oxidizing side of PS II). One approach to this problem is to use matrix algebra (Delrieu 1974), which resulted in '3-sigma analysis' (Lavorel 1976; Lavorel and Lemasson 1976) and '4-sigma analysis' (Thibault 1978; Meunier and Popovic 1989; Meunier and Popovic 1991). The strength of this approach is that in the initial steps, the fitted variables ('sigma coefficients' are determined without referring to a particular model (excepted that the 3-sigma analysis forces the sum of probabilities to be 100%, as per Kok's model). Because it separates the fittings and the interpretations the results from the fitting steps are not influenced by the investigator's preconceptions of the S-state mechanism. However, the sigma coefficients have to be interpreted to yield useful or meaningful results in terms of probabilities; direct interpretations of the 'sigma coefficients' have been limited to the framework of the original Kok model with three probabilities, thus losing one potential variable. Moreover, N more variables (the initial distribution of S-states) have been left undetermined so far by this approach. Some improvements were made to 'sigma analysis' by allowing photoactivation and photoinhibition with sums of probabilities different from 1 (Meunier and Popovic 1989; Meunier and Popovic 1991), at the loss of the capacity to predict the steady-state distribution of S-states.

By transforming the 'sigma coefficients' into eigenvalues, and interpreting the eigenvalues instead, we were able to retrieve a 4th probability, interpreted as backward transitions. We renamed that analysis the eigenvalue method, owing to its well-known mathematical foundation (Meunier 1993). However, the backward transition probability is homogeneous, whereas backward transitions are in reality produced by inhomogeneous deactivations in the interval between flashes; backward transitions are therefore only a loose approximation to the real phenomenon.

We propose improvements to the eigenvalue method that can account for: the presence of the S_{-1} state, explicit deactivations in the dark interval between flashes, inhomogeneous probabilities, and the change in the number of active PS II centers by photoinhibition or photoactivation. We also add the capacity to predict the steady-state distribution of S-states under conditions of steady photoinhibition or photoactivation, as well as the calculation of the initial S-state distribution. By these improvements to the eigenvalue method, we produced a model of the S-state mechanism that can be used with normal trial-and error fittings. These new tools allow us to deduce that double-hits encompassing the S_2 to S_3 transition are most likely negligible, and that true photochemical misses are much smaller than homogeneous fittings suggest.

Materials and methods

Strains and oxygen yield measurements

Cyanothece sp. ATCC 51142 was grown as previously described in ASP_2 medium without $NaNO_3$, with shaking at 100 rpm in 1 L flasks and under an illumination of roughly 50 $\mu E\ m^{-2}\ s^{-1}$ (Reddy et al. 1993). For subculture, stationary phase cultures were diluted to a concentration of 10^6 cells ml^{-1}, and log-phase cells were used for the experiments. *Synechocystis* sp. PCC 6803 wild-type and ΔpsbO cells were grown and maintained in BG-11 medium with additional nitrate ('6714' medium) as described previously (Burnap and Sherman 1991). O_2 flash yields were measured using a bare platinum electrode that allowed samples to be deposited upon the surface of the electrode by centrifugation in a Sorvall HB4-A swing-out rotor. The principle is similar to that described by Miyao et al. (1987), excepted that we used it with whole cells. The *Synechocystis* sp. PCC 6803 were centrifuged for 5 min on the electrode at 10000 rpm. The *Cyanothece* sp. ATCC 51142 cells (40 μg Chl) were harvested by centrifugation and resuspended in 200 μL of buffer

of the same osmolarity as the culture medium, but containing only 340 mM NaCl and 10 mM Hepes (pH 7.5). These 200 μL were then centrifuged 5 min at 1 K rpm on the electrode in a Sorvall HB4-A swing-out rotor. The slow centrifugation speed was essential to get a uniform layer of cells on the electrode. Absolute darkness during sample preparation (15 min total, including 5 on the unpolarized O_2 electrode) was required to maintain PS II activity. Between samples, the electrode was scrubbed with $NaHCO_3$ powder. Saturating xenon flashes were then used to advance the S-state mechanism. Signals were amplified using an electronic circuit based upon the design of Meunier and Popovic (1988). Oxygen yields were deconvoluted from respiratory transients as described in Meunier et al. (1995).

Definitions

The application of matrix algebra to the description of the S-state mechanism has already been partially addressed (Delrieu 1974; Lavorel 1976; Delrieu 1983). We have extended this description in terms of well-known eigenvalue and eigenvector mathematics, and have also considered 5-step mechanisms. The initial S-state distribution was represented by a column vector:

$$S_i = \begin{bmatrix} S_1 \\ S_0 \\ S_1 \\ S_2 \\ S_3 \end{bmatrix} \quad (1)$$

where the S_X represent the quantity of PS II centers in the corresponding S-states. The effect of a flash was represented by the N×N transition matrix T, which in theory contained all the transition probabilities from one S-state to another, and where N was 4 or 5. The oxygen production at flash 'n' was found by using the O_2 production vector 'P' defined as:

$$P = [0\ 0\ 0\ \gamma_2\ (\beta_3 + \gamma_3)] \quad (2a)$$

or

$$P = [0\ 0\ 0\ 0\ (\beta_3 + \gamma_3)] \quad (2b)$$

where $\gamma 2$ is the double-hit probability from S_2, $\gamma 3$ is the double-hit probability from S_3, and β_3 is the single-hit probability from S_3. The choice between Eqs. (2a) and (2b) depended on the presence of double-hits from S_2 in the model being considered. The oxygen produced at flash 'n' was then:

$$Y_n = PT^{n-1}S_i \quad (3)$$

where the symbols have the same significance as before. The initial distribution of S-states was expressed as the sum of the eigenvectors of the S-state transition matrix 'T':

$$S_i = \sum_{j=1}^{N} b_j E_j \quad (4)$$

where E_j represents the N eigenvectors of T and the b_j are constants. By definition of an eigenvector,

$$T^{n-1}\, E_j = \lambda_j^{n-1}\, E_j \quad (5)$$

where T is the S-state transition matrix, E_j is an eigenvector and λ is the corresponding eigenvalue. Combining Eqs. (3), (4) and (5) yields:

$$Y_n = \sum_{j-1}^{N} b_j \lambda_j^{n-1}\, PE_j \quad (6)$$

where the symbols have the same meaning as before. We defined new constants c_j as:

$$c_j = b_j\, PE_j \quad (7)$$

which yields Eq. (8) (see below).

Analytical methods

Equation (8) fitted oxygen yields down to the level of experimental noise:

$$Y_n = c_1\lambda_1^{n-1} + c_2\lambda_2^{n-1} + c_3\lambda_3^{n-1} + c_4\lambda_4^{n-1} + c_5\lambda_5^{n-1} \quad (8)$$

where Y_n is the oxygen yield on the nth flash, the c_j are constants used to determine the initial S-state distribution, and the λ_j are the eigenvalues of the S-state transition matrix. The fitting was best done by using mathematical computation packages such as Mathcad® (MathSoft, Inc.), which support complex calculus, because c_3, λ_3, c_4 and λ_4 were imaginary numbers. Since c_4 and λ_4 were, respectively, the complex conjugates of c_3 and λ_3, they were not independent variables and thus were not considered independently in the fitting procedure. Since there are 2N degrees of freedom in Eq. (8), a minimum of 2N flashes needed

to be used in the fitting, where N was 5. The fitting that we propose is different from fitting directly probabilities and initial S-state distributions. There needs to be a specific model and a specific set of assumptions employed to calculate oxygen yields in those fittings. By contrast, Eq. (8) doesn't assume a specific model; the only implicit approximation is that an N-step process with constant properties is involved. This separates the fitting process from the modeling step, an advantage that will be discussed later.

Once the constants c_j had been calculated by using one of the above methods, the initial distribution of S-states was found by transforming the constants according to this equation:

$$b_j = c_j \div (PE_j) \quad (9)$$

where the symbols have the same significance as before. The initial distribution of S-states was then found by using Eq. (4). In order to obtain the eigenvectors, a theoretical S-state transition matrix needed to be constructed, from which the eigenvectors were calculated automatically by Mathcad®. Therefore, the eigenvectors (but not the eigenvalues) depended on the model of the S-state transition matrix that was used. Consequently, a different initial distribution of S-states may be found for each model of the S-state mechanism. This situation exists also in the trial-and-error methods of directly adjusting the initial S-state distribution. However, those fitting procedures may include restraints such as 'The quantities of centers in any S-state must be real, positive numbers or be equal to zero.' This forces a feedback on the estimated transition probabilities that must be adjusted (i.e. distorted) to satisfy the constraints. Moreover, the placement of probabilities (i.e. if double-hits from S_2 are allowed in the model whereas almost none occur) will also feedback upon the estimated probabilities; in this case the estimated probability of double-hits will be made lower by the fitting program, whereas the other variables will be distorted in order to compensate. In the case of trial and error, each set of fitted variables is thus 'linked' to its theoretical model. The advantage of the method we propose is that the constants 'c_j' and the eigenvalues are determined without referring to any particular model. The fit is therefore the best possible one, and the subsequent process of finding the best model (the interpretation of the c_j and λ_j) is an independent process. This prevents the investigator's pre-conceptions from distorting the fitting process (it is a 'blind' fitting), and thereafter inferences can be made as to the validity of particular models based on their predicted initial distribution of S-states (see 'Results' and 'Discussion').

Under difficult conditions, it was easier to first find estimates of the eigenvalues by multivariable linear regression (see Appendix). Then, those estimates were used as starting points for the fit. This was numerically better because, in Eq. (8), an equal importance was given to all oxygen yields, which was not the case when multivariable regression analysis was used (as described in the Appendix). The residual standard deviation after fitting Eq. (8) was also a small fraction less than when using the multivariable linear regression, possibly due to the different weights of the O_2 yields and to cumulative numerical errors in the regression process.

Results

Necessity of the 5-step analysis

It has been repeatedly observed in several organisms that 4-step fittings perform better if the data on the first flash is ignored (Thibault 1978; Thibault and Thiéry 1981). However, in those cases 5-step fittings work significantly better, suggesting the presence of a 5th S-state, S_{-1} (Thibault 1982; Thibault and Thiéry 1981). In *Synechocystis* sp. PCC 6803, the same phenomenon is observed, as demonstrated by the typical O_2 production results shown in Fig. 1. In this figure, a 4-step fitting performed by the eigenvalue method, without the first flash, resulted in a significant disagreement between the predicted and the experimental O_2 yields on the first flash. By contrast, the experimental data was almost indistinguishable from a 5-step eigenvalue fitting that used the first flash. The eigenvalues help the understanding of this phenomenon (Table 1). The first column shows the eigenvalues from fitting the flashes 1–10; the first eigenvalue represents the ratio of active centers before and after each flash; the second eigenvalue is negative, and the third and fourth are complex conjugates, i.e. they are identical except for the sign of their imaginary parts (denoted by 'i') (Meunier 1993). By using 4-step fittings, with or without taking the first flash into account, and comparing their results in columns 1 and 2, it can be seen that the deduced properties of the S-state mechanism differed greatly (on the basis of the uncertainties in the 3rd column) if the first flash is taken into account. However, by using a 5-step analysis on flashes 1–10 (4th column), the first four eigenvalues were identical to those of col-

Table 1. Eigenvalues in *Synechocystis* sp. PCC 6803 'wild type' (glucose-tolerant). The flash numbers considered are indicated in parentheses, and the imaginary part of the eigenvalues is denoted by 'i'. The uncertainties over the eigenvalues are derived from the uncertainties given by the multivariable linear regression over the traces of the matrix (the 'sigma coefficients'; see the Appendix). They represent how well the model fits the data, but not how reproducible it is. There were no uncertainties for the 5-step analysis since there were no extra flashes above the minimum necessary to perform the multivariable linear regression

Eigenvalue	4-step (1–10)	4-step (2–10)	Uncertainties (2–10)	5-step (1–10)
λ_1	0.999	0.99638	0.00001	0.99641
λ_2	−0.67	−0.612	0.001	−0.611
λ_3	0.1631 + 0.717i	0.1563 + 0.7340i	0.0001 + 0.0001	0.1561 + 0.7339i
λ_4	0.1631 − 0.717i	0.1563 − 0.7340i	0.0001 + 0.0001	0.1561 − 0.7339i
λ_5	-	-	-	−0.01

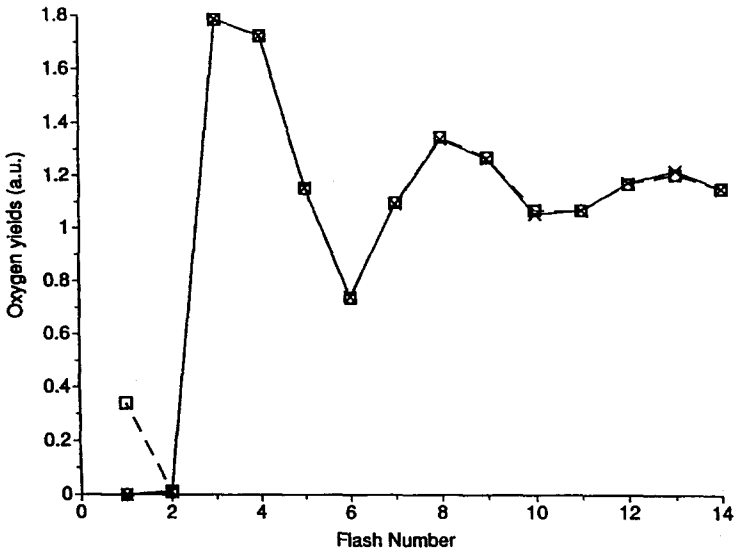

Fig. 1. Oxygen yields under flashing light in wild type *Synechocystis* sp. PCC 6803. The experimental data is represented by crosses (×); the 4-step fitting (using flashes 2–14) is shown by squares () and the 5-step fitting (using flashes 1–14) is shown by circles (○).

umn 2. This means that the 5-step analysis correctly took into account the information provided by the first flash, and that 4-step analyses done without taking the first flash into account correctly provided a subset of the properties of the S-state mechanism. We conclude that a 5-step analysis is the minimum necessary in the cyanobacterium *Synechocystis* sp. PCC 6803, and that eigenvalues are consistent variables for the description of the oxygen production mechanism. Similar results were obtained in the cyanobacterium *Cyanothece* sp. ATCC 51142 and the green alga *Dunaliella tertiolecta* (not shown). More complex analyses (6-step) may be necessary under different conditions, e.g. in the presence of exogenous reductants, but this will be addressed in a separate publication. The meaning of the fifth eigenvalue is addressed below.

The interpretation of eigenvalues and the initial S-state distribution

The interpretation of the eigenvalues is not limited to the homogeneous case of probabilities as described previously (Meunier 1993). We modeled the contribution of deactivations between flashes to apparent misses (Meunier and Popovic 1990) and to backward transitions (Meunier 1993) by using a deactivation matrix

Construction of the Models

Deactivation Matrix:

$$D(\delta)=\begin{bmatrix} 1 & 0 & 0 & 0 & 0 \\ 0 & 1 & 0 & 0 & 0 \\ 0 & 0 & 1 & \delta & \delta^2/2 \\ 0 & 0 & 0 & (1-\delta) & \delta-\delta^2/2 \\ 0 & 0 & 0 & 0 & (1-\delta) \end{bmatrix}$$

Forward Transition Matrix:

$$F(\alpha,\beta,\gamma,const[\varepsilon])=\begin{bmatrix} \alpha & \varepsilon & \varepsilon & \varepsilon & \varepsilon \\ \beta & \alpha & 0 & 0 & \beta \\ \gamma & \beta & \alpha & 0 & \gamma \\ 0 & \gamma & \beta+\gamma & \alpha & 0 \\ 0 & 0 & 0 & \beta+\gamma & \alpha \end{bmatrix}$$

A. Deactivation Model (D.F):

$$T(\alpha,\beta,\gamma,\delta,const[\varepsilon])=\begin{bmatrix} \alpha & \varepsilon & \varepsilon & \varepsilon & \varepsilon \\ \beta & \alpha & 0 & 0 & \beta \\ \gamma & \beta+\delta*\gamma & \alpha+\delta*(\beta+\gamma) & \alpha*\delta+(\beta+\gamma)*\delta^2/2 & \gamma+\alpha*\delta^2/2 \\ 0 & \gamma*(1-\delta) & (\beta+\gamma)*(1-\delta) & \alpha*(1-\delta)+(\delta-\delta^2/2)*(\beta+\gamma) & \alpha*(\delta-\delta^2/2) \\ 0 & 0 & 0 & (\beta+\gamma)*(1-\delta) & \alpha*(1-\delta) \end{bmatrix}$$

B. Deactivation Model with Double-Hits :

$$T(\alpha,\beta,\gamma,\delta,const[\varepsilon])=\begin{bmatrix} \alpha & \varepsilon & \varepsilon & \varepsilon & \varepsilon \\ \beta & \alpha & 0 & \gamma & \beta \\ \gamma & \beta+\gamma*\delta & \alpha+\delta*\beta+\gamma*\delta^2/2 & \alpha*\delta+\beta*\delta^2/2 & \gamma+\alpha*\delta^2/2 \\ 0 & \gamma*(1-\delta) & \beta*(1-\delta)+\gamma*(\delta-\delta^2/2) & \alpha*(1-\delta)+\beta*(\delta-\delta^2/2) & \alpha*(\delta-\delta^2/2) \\ 0 & 0 & \gamma*(1-\delta) & \beta*(1-\delta) & \alpha*(1-\delta) \end{bmatrix}$$

Fig. 2. Construction of the deactivation model. The matrices describe the effect of deactivations (D) and the effect of a flash (F) for the construction of the Deactivation Model. The result of a flash followed by a dark interval is then D*F; this is the apparent transition matrix T. The F matrix for the Deactivation Model with Double-Hits is not shown, but the D matrix is identical. The formulas were used to calculate the transition probabilities for the set of variables given in parenthesis, T(...). The quantity ε is written as *const*[ε] to underline the fact that for each automated fitting, ε was a constant. The significance of the variables α, β, δ and γ is described in the text. The matrices multiply the S-state vector (Eq. (1)) to yield the new S-state distribution after a flash. The first column applies to centers in S_{-1}; subsequent columns apply in order to centers in the other S-states. The first row lists the probabilities of centers in different S-states of effecting a transition ending in S_{-1}, and so on for subsequent rows.

(Fig. 2). The deactivation matrix 'D' uses the same probability for deactivations from S_2 and S_3, in order to limit the number of unknowns. This does not take into account the different stabilities of the S_2 and S_3 states, but is consistent with the presence of a fast deactivation phase in their biphasic kinetics (Styring and Rutherford 1987). The probability of a second deactivation, resulting in deactivations from S_3 to S_1, was calculated as $\delta^2/2$, for reasons previously discussed (Meunier 1993). No distinction is made as to the source of the electrons for the deactivations, and thus D also approximates roughly those produced by the effect of tyrosine Y_D of protein D2 (Vermaas et al. 1984).

The effect of each flash is represented by a 'forward' transition matrix F, that does not contain backward transitions. This matrix contains a new parameter, ε, that represents the entry of new centers in the S_{-1} state during photoactivation. This is not a perfect representation of reality since newly activated centers most likely start in the S_{-2} state. However, this is a significant improvement over having the sum of misses, single-hits and double-hits greater than 100%, which implied that newly activated centers could enter the S-state cycle in any state. The value of ε is calculated as follows. If the first eigenvalue is less than or equal to 1, then there is no photoactivation; in this case ε=0. If the first eigenvalue is greater than 1, then ε is given a value such that $\alpha+\beta+\gamma=1$. This value is approximately equal to λ_1-1 because we choose not to have ε apply to the S_{-1} state. This choice is of negligible or no consequence to the results, and other researchers using our model may have ε apply to the S_{-1} state if they so desire; however, our choice prevents a confusion between misses in S_{-1} and the activation of new centers, and provides formal consistency with our equivalent 6-step model (not shown). Because of the manner in which ε is calculated, it does not add to the number of independent variables. If photoinhibition is dominant, then ε is zero, and it is as if it did not exist. If ε is greater than zero, then it introduces the limitation $\alpha+\beta+\gamma=1$, which keeps the number of degrees of liberty to 3. Thus, the forward transition matrix has only three independent variables. This model also assumes that photoinhibition or any other loss

of active centers may occur in any S-state. In addition, double-hits encompassing the S_2 to S_3 transition were not allowed, for reasons to be made clear later. The question arises of what happens instead of double-hits from the states S_1 and S_2. When a second transition is not possible, then it is logical to assume that the result is a single-hit; this is why the single-hit probability is calculated as $(\beta + \gamma)$. Therefore, the variable γ is not limited to meaning double-hits in the Deactivation Model. The final transition matrix T is then the product D*F (Fig. 2).

As a result of multiplying D and F, misses were calculated as a homogeneous 'base' level representing 'true' photochemical misses, to which were added single-hits followed by deactivations from S_2 or S_3. True misses followed by a deactivations, or single-hits followed by two deactivations, constituted backward transitions. The result was a very inhomogeneous matrix that we will call the Deactivation Model. We also made a version of the deactivation model that allowed double-hits from S_1 or S_2, that we will call the Deactivation Model with Double-Hits (Fig. 2).

In Fig. 1, the oxygen yields on the third and fourth flash were almost equal, suggesting either that the $S_0Y_D^+$ population was large, or that the combination of misses, deactivations and the presence of reduced tyrosine Y_D of protein D2 (Vermaas et al. 1984) produced a retardation in the advancement of centers starting in the S_1 state. We analyzed these data with the 5-step homogenous model (not shown) and the two deactivation models (Table 2). Please note that in the deactivation models, the variables in Table 2 (α, β, γ, δ) do not represent the averaged transition probabilities, but are rather the parameters used to calculate the matrices as described in Fig. 2; thus, comparisons must take into account the difference in meaning. In the homogeneous model, the total (true + apparent) averaged miss probabilities were high (18%). By contrast, the true photochemical misses (represented by 'α') in the deactivation models were only 5%. The deactivation models returned a probability of deactivation of around 30% in the S_2 and S_3 states. Averaging the misses calculated from deactivations in Fig. 2 (the diagonal elements), gives a result almost identical to the averaged miss probability found by the homogeneous model. Thus, misses were resolved into 'true' and 'apparent' misses due to the effect of deactivations.

Moreover, the homogeneous model returned high quantities of S_0 (37%); the deactivation models returned only about 25%. Thus, the deactivation models were able to discriminate that some centers in S_1 had been slowed down by deactivations (whether from Y_D or other sources) and were not truly centers originally in S_0. The effect of Y_D was described as a one-time reduction (deactivation) of S_2 or S_3 (Vermaas et al. 1984; Styring and Ruthertord 1987); for this reason, our deactivation model only approximates this variable effect. Thus, under certain conditions, some centers in S_1 could still appear as starting in S_0 due to the effect of Y_D, despite the use of our deactivation models. Thus, we do not expect the initial distribution of S-states found by our model to be strictly invariant at different flash frequencies. Nevertheless, our models provide significant improvements.

The deconvolution also affected single-hits; the 'true' single-hit probability was higher in the deactivation models ('true' single-hits were calculated as $\gamma + \beta$ in some states of the Deactivation Model). This suggests a higher photochemical yield of PS II than is apparent from the homogeneous model. We propose that the higher miss probabilities commonly reported are due to the experimental conditions that allow deactivations in the dark interval between flashes, and not to an intrinsic inefficiency of the photochemical mechanism of PS II.

It is worth noting that the homogeneous model returned a value quite different from the experimental one for the fifth eigenvalue, λ_5, that was not fitted. This value was predicted much better by our deactivation models, despite the fact that they were fitted only to the first four eigenvalues and used only 4 variables in order to reproduce 5.

The improved eigenvalue approach allowed us to calculate the initial distribution of S-states from analytical equations (Table 2). A bothersome feature of homogeneous models is the finding of negative initial quantities of centers in the S_2 state (Table 2, column 1), as previously reported in the wild-type and the *psbO*-deletion mutant of *Synechococcus* PCC 7942 (Engels et al. 1994), in *Oscillatoria chalybea* (Bader 1989), in *Euglena gracilis* and to a lesser extent in *Chlorella vulgaris* (Schmid and Thibault 1983). We observed this phenomenon with all other models we tested, if the model included double-hits encompassing the S_2 to S_3 transition (not shown). This can be observed also by using the Deactivation Model with Double-Hits (Table 2, column 3). It appears that the modeling of double-hits encompassing the S_2 to S_3 transition is responsible for the apparently negative quantities of centers in the S_2 state. By contrast, our Deactivation Model (Table 2, column 2) finds a positive but small quantity of S_2.

Table 2. Interpretation of the eigenvalues found from the fitting depicted in Fig. 1, according to different models. We used the Mathcad® (MathSoft, Inc.) program to automatically adjust the probabilities and calculate the eigenvalues of T until a match with the first four experimental eigenvalues was found. The fifth eigenvalue, λ_5, was left to vary freely, and ε was zero; the experimental 5th eigenvalue was 0.03

		Model		
		Homogeneous	A (deactivation)	B(+double-hits)
Variables	α (misses)	17.8	5.4	5.6
(%)	β (single-hits)	76.8	88.6	91.9
	γ (double-hits)	2.5	5.7	2.1
	δ	2.7	30.2	30.7
Eigenvalue	λ_5	0.178	0.054	0.056
Initial	S_{-1}	6.3	5.6	5.7
distribution	S_0	36.6	24.3	25.5
(%)	S_1	62.1	69.8	72.6
	S_2	-5.1	0.28	-3.8
	S_3	0.19	0.00	0.09

Note that in the deactivation models, the variables α, β, γ and δ do not have the same meaning as in the homogeneous case. While in the homogeneous model, these are homogeneous probabilities, in the deactivation models they are parameters used to calculate the actual probabilities. The comparison is also complicated between the two deactivation models, because the variable γ was added to some single-hits in the Deactivation Model. To compare them, one should average the single-hits in matrix F, not taking deactivations into account: $[(88.6 + 88.6 + (88.6 + 5.7) + (88.6 + 5.7) + 88.6]/5 = 90.9$. The coefficient δ was the probability of backward transitions in the context of the homogeneous model, but is the probability of deactivations in the S_2 and S_3 states for the deactivation models. All models used flashes 1 to 14.

We conclude that double-hits encompassing the S_2 to S_3 transition must be negligible.

S-state properties of unstable manganese centers

Oxygen production from the *psbO* deletion mutant of *Synechocystis* sp. PCC 6803 usually shows a fast damping that makes the analysis very difficult (Engels et al. 1994; Burnap et al. 1992). Fully dark adapted cells show no or little oxygen production, as was noted previously after 5 h (Engels et al. 1994). However, we see an oxygen consumption on the first and second flashes, no oxygen on the third, and then small amounts that are progressively increasing (Fig. 3). The oxygen consumption is in agreement with the hypothesis that oxygen binding to Photosystem II is necessary before it can evolve oxygen (Bader et al. 1987). However, we recently showed how respiratory transients are produced by Photosystem I and II activities in *Synechocystis* sp. PCC 6803 (Meunier et al. 1995). Thus, the initial oxygen consumptions could be the result of non-O_2 evolving PS II activity that reduced the plastoquinone pool and stimulated cytochrome oxidase activity. A distinction between those possibilities should be possible for researchers having access to a mass spectrometer.

After 3 min under a 10 Hz flash regime (not shown), the same sample showed a greatly enhanced oxygen production activity (Fig. 3). Yet after a subsequent dark-adaptation this activity was lost again (not shown). Due to this instability of the manganese centers, the analysis of oxygen yields after a full 'dark adaptation' is not possible and the dark incubation time must be kept short. In addition, the damping of the pattern was often too quick even after photoactivation for a reliable analysis. By letting cells adapt to 4 °C in the light, an increased stability in the dark could be observed, accompanied by sustained oscillations of oxygen production (Fig. 4). This increased stability may have two contributing factors. A direct effect of temperature upon the recombination rate of charges, such as that governing the use of thermolumi-

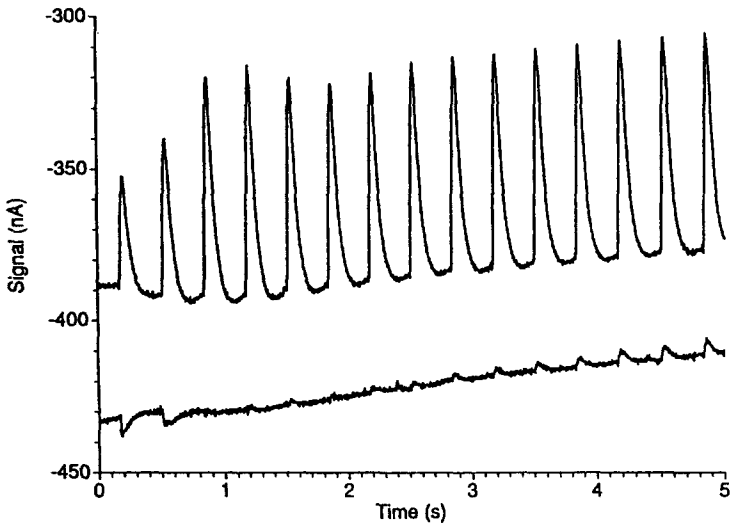

Fig. 3. Time course of the oxygen electrode signals for two experiments in the *psbO* deletion mutant of *Synechocystis* sp. PCC 6803. The two experiments were performed on the same sample. The first experiment was performed after a dark-adaptation period of 7 h total (lower line); the cells were dark-adapted in their growth medium, with air bubbling, and centrifuged onto the electrode just before the experiment. Flashes were given at a frequency of 3 Hz starting 167 ms after the experiment was started. Between the first and second experiments, flashes were given at a 10 Hz frequency for 3 min without recording the signal. After a delay of 10 s, flashes were given again at a frequency of 3 Hz while recording the signal. The oxygen signal from the same sample (partially reactivated *psbO* deletion mutant of *Synechocystis* sp. PCC 6803) is shown in the upper trace (shifted vertically for clarity).

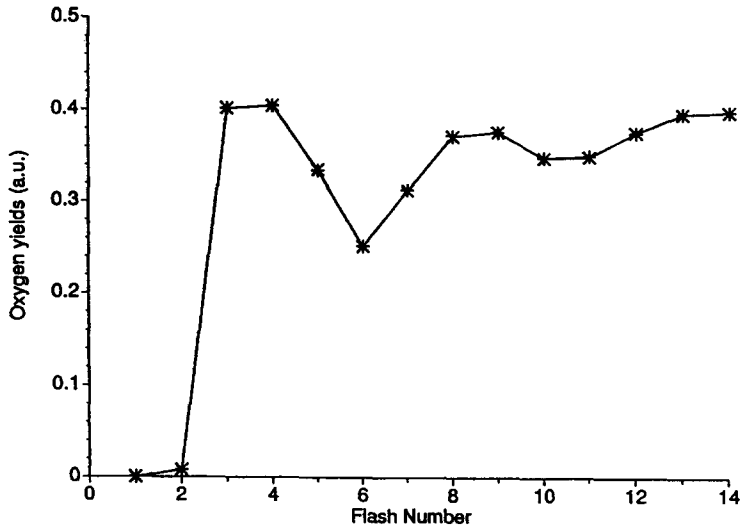

Fig. 4. Oxygen yields under flashing light in the *psbO* deletion mutant of *Synechocystis* sp. PCC 6803 incubated at 4 °C in the light for 2 h. The experimental data is represented by crosses (×); the 5-step fitting (using flashes 1–14) is shown by the plus sign (+). Flashes were given at a frequency of 3 Hz starting 167 ms after the experiment was started.

nescence, is possible; this would lower misses caused by deactivations. However, due to the tight interaction between respiratory and photosynthetic electron flows in cyanobacteria, another contribution was from an inhibition of respiration at that temperature, that resulted in a more oxidized state of the plastoquinone pool (not shown), which decreased the amount of available reductants for the deactivation of S-states. It should be noted that while the S_3 and S_2 states were found to be more stable in the mutant than in the wild-type (Engels et al. 1994; Burnap et al. 1992), deactivations

also happen from the S_1 and S_0 states since the mutant looses activity in the dark.

The data in Fig. 4 resembles somewhat that reported previously for the *psbO* deletion mutant of *Synechocystis* sp. PCC 6803; however, our results show comparable yields on the third and fourth flashes and a slower damping, while previously the fourth flash was significantly higher (Engels et al. 1994). We believe that this is due to the lower temperature. An upward trend in the flash sequence clearly indicates that photoactivation is significant and that λ_1 is greater than 100%. If one adds up the S-state transition probabilities previously reported (Engels et al. 1994), it can be seen that the sum is significantly greater than 100% in the *psbO* deletion mutants, although this wasn't discussed in the publication. Thus, photoactivation needs to be taken explicitly into account in these strains, and we propose to do so by using the probability 'ε'.

Our data was analyzed with the Deactivation Model (Table 3). As expected, we found that λ_1 was significantly greater than 1. The probability of deactivations from S_2 and S_3 was lower than it the wild type, also in accordance with previous results (Engels et al. 1994; Burnap et al. 1992). However, the miss probability was significantly lower than that previously reported (34%) (Engels et al. 1994). We believe that this is due to the effect of deactivations, that previously added to misses, while we explicitly and separately took them into account. However, there were still more true misses in the mutant than in the wild type (Table 3). We conclude that the photochemical efficiency of PS II in the mutant is truly lowered, and that the higher misses in the mutant are not simply due to more deactivations in the dark intervals. This is in agreement with previous biochemical results in higher plants (Miyao et al. 1987).

In addition, we report on a wild-type cyanobacterium, *Cyanothece* sp. ATCC 51142, that fixes nitrogen in cycles that display the phenotypic behavior of circadian rhythms (Reddy et al. 1993; Schneegurt et al. 1994). When cultures are grown in the absence of combined nitrogen, either under 12 h light/12 h dark cycles or in continuous light, the cells fix N_2 with peaks every 24 h. The rates of steady-state oxygen evolution assayed during this cycle decreased during the dark phase, especially during nitrogen fixation peaks (M.S. Colon-Lopez and L.A. Sherman, unpublished data). In addition, *Cyanothece* sp. ATCC 51142 demonstrated a reversible instability of manganese during the light period that is similar to that of the *psbO* deletion mutant of *Synechocystis* sp. 6803 (Fig. 5). The first experiment after a dark adaptation (15 min), 4 h into the light period (L4) showed a highly dampened sequence with a clear, progressive increase in the oxygen yields as centers were photoactivated. A complete analysis was not possible with this sequence, but the value of λ_1 could still be retrieved (1.043). However, a photoactivation treatment followed by a brief dark adaptation of 30 s produced higher oxygen yields that could be analyzed successfully.

The oxygen yields in Cyanothece sp. ATCC 51142 at 4 hours into the light period (L4), after a photoactivation treatment, were analyzed with the Deactivation Model (Table 3). The photoactivation treatment lowered λ_1 to less than 1, which indicates that no more centers could be reactivated after 3 min of 10 Hz flashes. The results show a high probability of deactivations in S_3 and S_2 but a low probability of misses, showing that the instability of manganese in this organism is not linked to an intrinsic inefficiency of Photosystem II, but rather to an astonishing reversibility of the reactions involved. These properties are also opposite of those brought about by the loss of the PsbO protein. This suggests that the instability of manganese is not linked to a missing PsbO protein under those conditions, but rather that this instability is an integral part of the regulation mechanism of PS II activity in *Cyanothece* sp. ATCC 51142. However, this does not rule out differences in the PsbO protein that would allow for these properties.

We also analyzed the properties of oxygen yields in *Cyanothece* sp. ATCC 51142 at 2.5 h into the dark period (D2. 5, Fig. 6). These samples were in the dark for several hours before the experiment; yet the pattern shows a clear oscillation with maximum on the fourth flash, and little photoactivation is visible. It can be seen that the properties of O_2 production are not constant in this wild-type diazotrophic organism; this will be discussed in detail in an upcoming publication (Meunier et al., unpublished data). The analysis with the Deactivation Model (Table 3) showed higher miss and double-hit probabilities; at this time we have no explanation for the higher double-hit probability. The probability of deactivations remained about the same, and a slight photoactivation could be detected ($\lambda_1 = 1.004$). A noticeable difference with the wild-type *Synechocystis* sp. PCC 6803 is the presence of important quantities of centers in the S_{-1} state.

From Table 3, it can be seen that the fifth eigenvalue was predicted accurately (well within the uncertainties) by our model. Our method also offers a convenient way of calculating the steady-state distribution

Table 3. Analysis of O_2 yield sequences with the Deactivation Model. *Cyanothece* sp. ATCC 51142 was measured 2.5 h into the dark period (D2.5) and 4 h into the light period (L4), after a photoactivation treatment

		Cyanothece sp. ATCC 51142		*Synechocystis* sp. PCC 6803 *psbO*	
		D2.5	L4	Deletion	Wildtype
Variables	α	6.9	2.0	16.7	5.4
(%)	β	77.9	95.4	76.3	88.6
	γ	15.2	2.4	7.1	5.7
	δ	32.4	34.7	10.1	30.2
Const	ε	0.4	0.0	2.4	0.0
Eigenvalues	λ_1	1.004	0.998	1.0240	0.998
		+/−0.003	+/−0.002	+/−0.0007	+/−0.002
Predicted	λ_5	0.07	0.02	0.14	0.054
Observed	λ_5	0.09+/−0.3	0.1+/0.3	0.15+/−0.04	0.0+/−0.3
Initial	S_{-1}	18.1	2.7	22.2	5.6
distribution	S_0	26.1	18.5	23.7	24.3
(%)	S_1	55.1	42.3	53.3	69.8
	S_2	0.66	28.6	0.85	0.28
	S_3	0.00	7.9	0.00	0.00
Steady-state	S_{-1}	0.4	0.0	2.7	0.0
distribution	S_0	17.3	18.8	22.6	19.1
(%)	S_1	31.1	32.2	25.6	30.8
	S_2	30.9	29.7	26.4	29.7
	S_3	20.3	19.3	22.7	20.4

The S-state distributions and probabilities are in percent. The experiments were analyzed using flashes 1–14 excepted for L4 which used 1–13. 'Glitches' or noise that resulted in a significantly worse (residual standard deviations higher by factors greater than 2) fitting upon including a flash in the analysis occurred randomly. While some were obvious enough to discard the experiment outright, some could not be detected until a fitting was attempted, which is why the 14th flash was not considered at L4.

of S-states; the eigenvector for the first eigenvalue, already calculated for the initial distribution, is proportional to the steady-state distribution (Table 3). It is interesting that all the distributions predicted by our model show $(S_2)\approx(S_1)>(S_3)\approx(S_0)$, especially in relation to the distribution $(S_2)>(S_1)>(S_3)\approx(S_0)$ observed in *Chlorella pyrenoidosa* (Lavorel and Maison-Peteri 1983). An interesting consequence of having steady photoactivation phenomena is the presence of centers in S_{-1} in the steady state. These are newly activated centers.

Discussion

The interpretation of eigenvalues is flexible and not limited to the homogeneous case of probabilities, or to the models we proposed. By fitting the eigenvalues, we found that incorrect models predict negative S-state distributions or negative probabilities. The deactivation model was successful in modeling the known properties of the S-state mechanism. Directly fitting the deactivation model to data by trial and error is likely to yield the very same results as the eigenvalue method; we see the eigenvalue method as most useful when trying or designing new models. This is due to the two-step nature of the eigenvalue analysis. The first step is the requirement that the eigenvalues of the

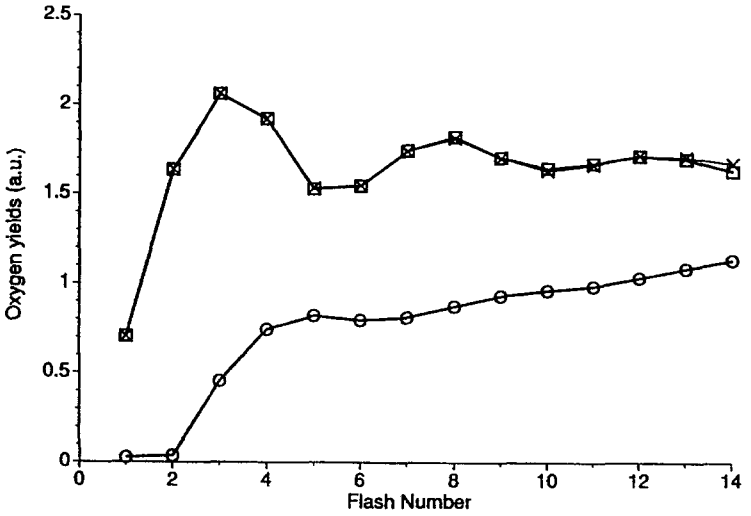

Fig. 5. Oxygen yields for *Cyanothece* sp. ATCC 51142 grown in nitrogen deficient media, at 4 h during the 12 h light phase. The first experiment after dark adaptation is shown by circles (○). Following a photoactivation treatment of 3 min of 10 Hz flashes and 30 sec dark adaptation, the experiment was repeated on the same sample. The experimental data is represented by squares (□); the 5-step fitting (using flashes 1–13) is shown by crosses (×). Flashes were given at a frequency of 3 Hz. The photoactivation treatments were done through a red filter similar to RG-610.

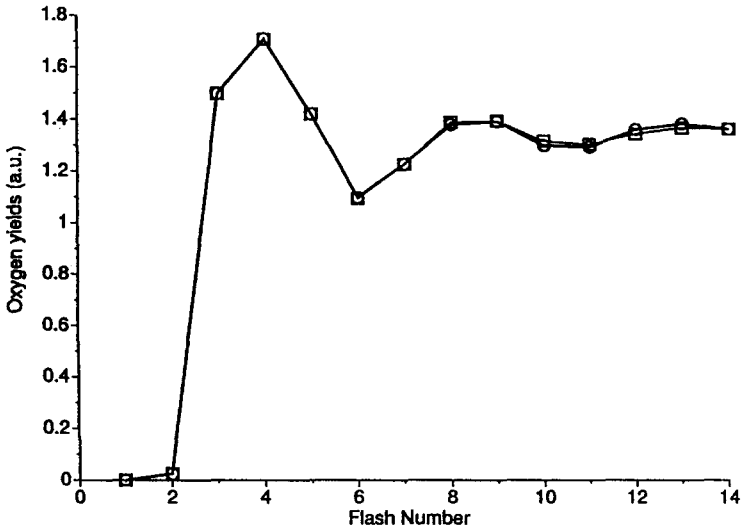

Fig. 6. Oxygen yields for *Cyanothece* sp. ATCC 51142 grown in nitrogen deficient media, at 2.5 h during the 12 h dark phase. Flashes were given at a frequency of 3 Hz. The experimental data is shown by circles (○); the 5-step fitting (using flashes 1–14) is shown by squares (□).

new model match the experimental eigenvalues. Then, the initial S-state distribution obtained from the model must satisfy requirements such as having only real, positive quantities. In this regard, we should mention that O_2 yields sequences produced by the bi-cycle model (Shinkarev et al. 1994) were undistinguishable from sequences with the averaged transition probabilities, such that the bi-cycle model could not unambiguously fit the data.

It is now possible to calculate the initial distribution of S-states with analytical equations. We presented an attempt to assess the validity of different S-state models based on the initial distribution of S-states that they predict. Our results suggested that there were negligible probabilities of double-hits encompassing the S_2 to

S_3 transition. This is consistent with the observation that the S_2 to S_3 transition does not saturate easily as a function of the light intensity (Delrieu 1980). In addition, no double-hits were detected in the first flash in *Chlorella* (Delrieu 1980), and double-hits from S_1 to S_3 were proposed to be nil (Delrieu 1983). The S_2 to S_3 transition was proposed to involve a reorganization of the electronic configuration and nuclear geometry of manganese (Messinger et al. 1991). By contrast, the transition of S_2 to S_3 was proposed to be special by not involving a change in the redox state of manganese (M. Haumann, W. Drevenstedt and W. Junge, abstract of the Xth international Congress on Photosynthesis). No matter which proposal is correct, it emerges that the S_2 to S_3 transition has special properties. The combination of these observations and proposals justifies our model with negligible double-hits involving the S_2 to S_3 transition.

A measured steady-state distribution of S-states $(S_2)>(S_1)>(S_3)\approx(S_0)$ was given as the basis for the proposal of a C/C^{++} auxiliary charge carrier and the rejection of the $S_3\rightarrow S_2\rightarrow S_1$ deactivation scheme in *Chlorella pyrenoidosa* (Lavorel and Maison-Peteri 1983). However, our model using such a $S_3\rightarrow S_2\rightarrow S_1$ deactivation scheme predicted distributions of the type $(S_2)\approx(S_1)>(S_3)\approx(S_0)$. The predicted quantities of steady-state S_2 and S_1 were almost equal because the deactivation probabilities in S_3 and S_2 were assumed to be equal in order to simplify the model; however, a distribution of the type $(S_2)>(S_1)>(S_3)\approx(S_0)$ would have been predicted if the S_3 state was given a higher probability of deactivation than the S_2 state. Thus, a slightly modified deactivation model could account for these observations.

Our deactivation model provides high misses in the S_1 and S_2 state. High misses in the S_2 state were proposed previously, but the proposed mechanism for these misses involved an 'inactive' special form of the S_2 state (Delrieu 1974; Delrieu 1983). We showed that high apparent misses in the S_2 state can be explained by the known properties of the S-state mechanism without postulating an additional (inactive) S_2 state of manganese, but we also added high misses in the S_1 state. As described above, misses in the S_2 state could be higher than in the S_1 state if the deactivation probabilities were higher in the S_3 state.

In accordance with other results (Thibault 1982; Bader et al. 1983; Engels et al. 1994; Schmid and Thibault 1983), we found that the S_{-1}, state may occur in vivo in appreciable quantities without the addition of exogenous reductants like hydroxylamine. We also found this to happen in a wild-type organism, *Cyanothece* sp. ATCC 51142. The presence of super-reduced S-states in appreciable quantities seems linked to the capacity for inactivation/reactivation reactions of PS II centers. It has been shown previously that *Euglena gracilis* has large quantities of S_{-1} in the dark (Schmid and Thibault 1983) and this organism is subject to loss of oxygen production capacity in the dark. *Cyanothece* sp. ATCC 51142 and the *psbO* deletion mutant of *Synechocystis* sp. PCC 6803 have significant quantities of centers in S_{-1} state and both undergo inactivation and reactivation phenomena. The same was observed in mutants of CP-47 (Gleiter 1995). Our results were consistent with the notion that the deletion of the MSP (manganese-stabilizing protein), although it stabilizes the S_3 and S_2 states (Burnap et al. 1992), actually destabilizes the S_0 and S_1 states thus permitting the appearance of large quantities of S_{-1} (and probably S_{-2}).

The instability of the manganese complex in cyanobacterial mutants (Engels et al. 1994; Gleiter et al. 1995) and a few wild-types so far, and the fast reactivation phenomena, result in special problems not found in most other strains or species. The normal Kok model or its extension to S_{-1} or S_{-2} cannot account for these phenomena. In this context, the use of our model (and its extension to a 6-step mechanism), or a similar one, is critical.

In conclusion, we have integrated well-documented features of the S-state mechanism such as backward transitions, the control of apparent misses by the redox state of plastoquinone through deactivations, inhomogeneous miss probabilities, observed steady-state distributions, the lack of double-hits on some S-states, photoinhibition ($\lambda_1<100\%$), photoactivation (ε), and to some extent the effect of Y_D into a self consistent 5-step model (the deactivation model) with manageable numbers of unknowns. We hope these will be useful tools for other researchers in photosynthesis.

Appendix: Error Analysis

The disadvantage of fitting Eq. (8) is that no error analysis is available. The second approach to determining the 'c_j' and the eigenvalues is to first find the eigenvalues, and then the 'c_j' by using multivariable linear regression. In the case of a 4-step process, the eigenvalues are found as described previously (Meunier 1993). The eigenvalue method can be extended to a 5-step process by writing the recurrence relation of

oxygen production as:

$$Y_{n+5} + a_1 Y_{n+4} + a_2 Y_{n+3} + a_3 Y_{n+2} + a_4 Y_{n+1} + a_5 Y_n = 0 \quad \text{(A1)}$$

where the a_i are the traces of the 5-step S-state transition matrix (e.g. the determinant is the 5th trace). The traces were also called 'sigma coefficients', from the first presentation of a similar equation. Note that the traces do not have the same values as they had in the four-step process, and previous definitions in terms of transition probabilities do not hold. As for the 4-step analysis, the first part of the analysis is to find the traces, by inverting the following equation by multivariable linear regression:

$$\begin{bmatrix} Y_{n+4} & Y_{n+3} & Y_{n+2} & Y_{n+1} & Y_n \\ Y_{n+5} & Y_{n+4} & Y_{n+3} & Y_{n+2} & Y_{n+1} \\ Y_{n+6} & Y_{n+5} & Y_{n+4} & Y_{n+3} & Y_{n+2} \\ Y_{n+7} & Y_{n+6} & Y_{n+5} & Y_{n+4} & Y_{n+3} \\ Y_{n+8} & Y_{n+7} & Y_{n+6} & Y_{n+5} & Y_{n+4} \end{bmatrix} \begin{bmatrix} a_1 \\ a_2 \\ a_3 \\ a_4 \\ a_5 \end{bmatrix} = \begin{bmatrix} -Y_{n+5} \\ -Y_{n+6} \\ -Y_{n+7} \\ -Y_{n+8} \\ -Y_{n+9} \end{bmatrix} \quad \text{(A2)}$$

The inversion is obtained through the following standard calculation for multivariable regression:

$$A = (X' * X)^{-1} * X' * Y \quad \text{(A3)}$$

where A is the column vector containing the traces, X is the matrix on the left side of Eq. (A2), X′ is its transpose, and y is the column vector on the right side of Eq. (A2).

The second part of the analysis is, as with the 4-step analysis, to write the characteristic equation of the S-state transition matrix using the traces:

$$\lambda^5 + a_1\lambda^4 + a_2\lambda^3 + a_3\lambda + a_5 = 0 \quad \text{(A4)}$$

where λ may have 5 values (eigenvalues) for which the equation holds. Four of those are exactly the same as for the 4-step analysis, and average probabilities of misses and single-hits, and the estimated probabilities of double-hits and backward transitions may be found with the same straightforward equations if so desired (Meunier 1993). Note, however, that those probabilities do not apply to the state S_{-1} (e.g. the average miss probability is the average only over the states S_0 to S_3). The fifth eigenvalue is often a small positive number, and under conditions where deactivations from S_0 to S_{01} do not occur, the fifth eigenvalue is equal to the probability of misses in S_{-1}. However, because it is an ill-defined number with extremely large uncertainties (typically 100% of its value), the eigenvalue may sometimes be negative.

once the eigenvalues have been found, the c_j can be determined by multivariable linear regression. The equation to be inverted, given here for the 5-step analysis (it can easily be simplified for the 4-step analysis), is:

$$\begin{bmatrix} \lambda_1^{n-1} & \lambda_2^{n-1} & \lambda_3^{n-1} & \lambda_4^{n-1} & \lambda_5^{n-1} \\ \lambda_1^{n} & \lambda_2^{n} & \lambda_3^{n} & \lambda_4^{n} & \lambda_5^{n} \\ \lambda_1^{n+1} & \lambda_2^{n+1} & \lambda_3^{n+1} & \lambda_4^{n+1} & \lambda_5^{n+1} \\ \lambda_1^{n+2} & \lambda_2^{n+2} & \lambda_3^{n+2} & \lambda_4^{n+2} & \lambda_5^{n+2} \\ \lambda_1^{n+3} & \lambda_2^{n+3} & \lambda_3^{n+3} & \lambda_4^{n+3} & \lambda_5^{n+3} \\ \lambda_1^{n+4} & \lambda_2^{n+4} & \lambda_3^{n+4} & \lambda_4^{n+4} & \lambda_5^{n+4} \\ \lambda_1^{n+5} & \lambda_2^{n+5} & \lambda_3^{n+5} & \lambda_4^{n+5} & \lambda_5^{n+5} \\ \lambda_1^{n+6} & \lambda_2^{n+6} & \lambda_3^{n+6} & \lambda_4^{n+6} & \lambda_5^{n+6} \\ \lambda_1^{n+7} & \lambda_2^{n+7} & \lambda_3^{n+7} & \lambda_4^{n+7} & \lambda_5^{n+7} \\ \lambda_1^{n+8} & \lambda_2^{n+8} & \lambda_3^{n+8} & \lambda_4^{n+8} & \lambda_5^{n+8} \end{bmatrix} \begin{bmatrix} C_1 \\ C_2 \\ C_3 \\ C_4 \\ C_5 \end{bmatrix} = \begin{bmatrix} Y_n \\ Y_{n-1} \\ Y_{n+2} \\ Y_{n+3} \\ Y_{n+4} \\ Y_{n+5} \\ Y_{n+6} \\ Y_{n+7} \\ Y_{n+8} \\ Y_{n+9} \end{bmatrix} \quad \text{(A5)}$$

which can be inverted to find the c_j in the same manner that Eq. (A3) inverted Eq. (A2). Only five rows are necessary; but, since ten flashes were used to find the eigenvalues, the same number was used to find the c_j for the sake of consistency. Taking all ten flashes into account also provides the basis for the calculation of uncertainties over the initial S-state distribution. Each time a multivariable linear regression is used, it is possible to find estimates of errors over the determined variables. The first step of the error analysis is to find the covariance matrix:

$$COV = (X' * X)^{-1} * s^2 \quad \text{(A6)}$$

where *COV* is the covariance matrix, s^2 is the residual variance after the fit, and X, X' have the same meaning as in Eq. (A3). Let us call the left side of Eq. (A4) 'f(λ)'. The variance of f(λ) the due to the variance of the traces is:

$$V(\lambda_j) + |E(\lambda_j)*COV*E(\lambda_j)'| \quad \text{(A7)}$$

where v(λ) is the variance around zero of f(λ) for a given eigenvalue λ_j, due to the variance of the traces; E(λ) is a horizontal vector having powers of λ as its elements. E(λ) is such that when it multiplies the vector of the traces found by Eq. (A3), it reconstitutes part of

Eq. (A4) and the result is equal to $f(\lambda)$-λ^5 (here shown for a 5-step mechanism):

$$E(\lambda_j) = [\lambda_j^4\ \lambda_j^3\ \lambda_j^2\ \lambda_j\ 1] \qquad (A8)$$

The standard deviation on each eigenvalue λ_j, $\sigma(\lambda_j)$, is then:

$$\sigma(\lambda_j) = \sqrt{\nu(\lambda_j)}/\left(\frac{df(\lambda)}{d\lambda}|_{\lambda=\lambda_j}\right) \qquad (A9)$$

where the denominator is the absolute value of the derivative of $f(\lambda)$ relative to λ, and is evaluated at $\lambda = \lambda_j$. The uncertainty over the 4 estimated average S-state transition probabilities can then be calculated by summing the squares of the first four standard deviations corresponding to λ_{1-4}:

$$\sigma_{\alpha,\beta,\gamma,\delta} = \frac{\sqrt{\sum_{j=1}^{4}\sigma^2(\lambda_j)}}{4} \qquad (A10)$$

where $\sigma_{\alpha,\beta,\gamma,\delta}$ represent the standard deviation associated with the estimated transition probabilities over the states S_0 to S_3. This last equation overestimates the standard deviations because it does not take into account the covariances between each S-state transition probability. We deduced similar equations for finding uncertainties on the initial distribution of S-states (not shown); however, in our experience, the assumptions that need to be made in order to find the initial distribution are a much greater source of variability. All the equations above may be extended to the case of 6-step analyses.

Acknowledgements

This research was supported by grants from the U.S. Department of Energy (DE-FG02-89ER14028) and from the US Department of Agriculture (93-37306-9238) to Dr L.A. Sherman.

References

Bader KP (1989) Alkylbenzyldimethylammonium chloride, a stabilizer of the S-state system in the flamentous cyanobacterium *Oscillatoria chalybea*. Biochim Biophys Acta 975: 399–402

Bader KP, Thibault P and Schmid GH (1983) A study on oxygen evolution and on the S-state distribution in thylakoid preparations of the filamentous blue-green alga *Oscillatoria chatybea*. Z Naturforsch 38c: 778–792

Bader KP, Thibault P and Schmid GH (1987) Study on the properties of the S_3-state by mass spectnometry in the filamentous cyanobacterium *Oscillatoria chalybea*. Biochim Biophys Acta 893: 564–571

Burnap RL and Sherman LA (1991) Deletion mutagenesis in *Synechocystis* sp. PCC 6803 indicates that the Mn-stabilizing protein of Photosystem II is not essential for O_2 evolution. Biochem 30: 440–446

Burnap RL, Shen JR, Jursinic PA, Inoue Y and Sherman LA (1992) Oxygen yield and thermoluminescence characteristics of a cyanobacterium lacking the manganese-stabilizing protein of Photosystem II. Biochem 31: 7404–7410

Delrieu MJ (1974) Simple explanation of the misses in the cooperation of charges in photosynthetic O_2 evolution. Photochem Photobiol 20: 441–454

Delrieu MJ (1980) Light intensity saturation properties of O_2 yields in a sequence of flashes in *Chlorella*. Biochim Biophys Acta 592: 478–494

Delrieu MJ (1983) Evidence for unequal misses in oxygen flash yield sequences in photosynthesis. Z Naturforsch 38c: 247–258

Delrieu MJ and Rosengard F (1987) Comparative study of period 4 oscillations of the oxygen and fluorescence yield induced by a flash series in inside out thylakoids. Biochim Biophys Acta 892: 163–171

Engels DH, Lott A, Schmid GH and Pistorius EK (1994) Inactivation of the water-oxidizing enzyme in manganese stabilizing protein-free mutant cells of the cyanobacteria *Synechococcus* PCC 7942 and *Synechocystis* PCC 6803 during dark incubation and conditions leading to photoactivation. Photosynth Res 42: 227–244

Forbush B, Kok B and McGloin M (1971) Cooperation of charges in photosynthetic O_2, evolution-2. Damping of flash yield oscillation, deactivation. Photochem Photobiol 14: 307–321

Gleiter HM, Haag E, Shen JR, Eaton-Rye JJ, Seeliger AG, Inoue Y, Vermaas WFJ and Renger G (1995) Functional characterization of mutant strains of the cyanobacterium *Synechocystis* sp. PCC 6803 lacking short domains within the large, lumen-exposed loop of the chlorophyll protein CP-47 in Photosystem II. Biochem 34: 6847–6856

Joliot P, Barbieri G and Chabaud R (1969) Un nouveau modèle des centres photochimiques du système II. Photochem Photobiol 10: 309–329

Kok B, Forbush B and McGloin M (1970) Cooperation of charges in photosynthetic O_2 evolution-1. A linear four step mechanism. Photochem Photobiol 11: 457–475

Lavorel J (1976) Matrix analysis of the oxygen evolving system of photosynthesis. J Theor Biol 57: 171–185

Lavorel J and Lemasson C (1976) Anomalies in the kinetics of photosynthetic oxygen emission in sequences of flashes revealed by matrix analysis. Biochim Biophys Acta 430: 501–516

Lavorel J and Maison-Petesi B (1983) Studies of deactivation of the oxygen-evolving system in higher plant photosynthesis. Physiol Vég 21: 509–517

Messinger J and Renger G (1993) Generation, oxidation by the oxidized form of the tyrosine of polypeptide D2, and possible electronic configuration of the redox states S_0, S_{-1} and S_{-2} of the water oxidase in isolated spinach chloroplasts. Biochem 32: 9379–9386

Messinger J, Wacker U and Renger G (1991) Unusual low reactivity of the water oxidase in redox state S_3 toward exogenous reductants. Analysis of the NH_2OH- and NH_2NH_2-induced modifications of flash-induced oxygen evolution in isolated spinach thylakoids. Biochem 30: 7852–7862

Meunier PC (1993) Oxygen evolution in Photosystem II: The contribution of backward transitions to the anomalous behaviour of double-hits revealed by a new analysis method. Photosynth Res 36: 111–118

Meunier PC and Popovic R (1988) High-accuracy oxygen polarograph for photosynthetic systems. Rev Sci Instrum 59: 486–491

Meunier PC and Popovic R (1989) Evidence for a linear variation of the miss and single-hit S-state probabilities with the flash number, measured by oxygen evolution in *Dunaliella tertiolecta*. Photosynth Res 22: 131–136

Meunier PC and Popovic R (1990) Control of misses on oxygen evolution by the oxido-reduction state of plastoquinone in *Dunaliella tertiolecta*. Photosynth Res 23: 213–221

Meunier PC and Popovic R (1991) Improvement of four sigma analysis for the investigation of oxygen of evolution by Photosystem II. Photosynth Res 29: 113–115

Meunier PC, Burnap RL and Sherman LA (1995) Interaction of the photosynthetic and respiratory electron transport chains producing slow O_2 signals under flashing light in *Synechocystis* sp. PCC 6803. Photosynth Res 45: 31–40

Miyao M, Murata N, Lavorel J, Maison-Peteri B, Boussac AGP and Etienne A-L (1987) Effects of the 33-kDa protein on the s-state transitions in photosynthetic oxygen evolution Biochim Biophys Acta 890: 151–159

Reddy KJ, Haskell JB, Sherman DM and Sherman LA (1993) Unicellular, aerobic nitrogen-fixing cyanobacteria of the genus *Cyanothece*. J Bacteriol 175: 1284–1292

Schmid GH and Thibault P (1983) Studies on the S-state distribution in *Euglena gracilis*. Z Naturforsch 38c; 60–66

Schneegurt MA, Sherman DM, Nayar S and Sherman LA (1994) Oscillating behavior of carbohydrate granule formation and dinitrogen fixation in the cyanobacterium *Cyanothece* sp. strain ATCC 51142. J Bacteriol 176: 1586–1597

Shinkarev VP and Wraight CA (1994) Oxygen evolution in Photosynthesis: From unicycle to bicycle. Proc Natl Acad Sci USA 90: 1834–1838

Styring S and Rutherford AW (1987) In the oxygen-evolving complex of Photosystem II the S_0 state is oxidized to the S_1 state by D^+ (signal II_{slow}). Biochem 26: 2401–2405

Thibault P (1978) A new attempt to study the oxygen evolving system of photosynthesis: Determination of transition probabilities of a state *i*. J Theor Biol 73: 271–284

Thibault P (1982) Contribution à l'étude des propriétés de l'émission photosynthétique d'oxygène. Recherche d'un modèle cohérent. PhD thesis, Université d'Aix-Marseille II (France)

Thibault P and Thiéry JM (1981) Modélisation de l'émission d'oxygène photosynthétique sous éclairs périodiques. In: Le Guyader H and Moulin T (eds) Actes du Premier Séminaire de l'Ecole de Biologie Théorique du Centre National de la Recherche Scientifique, pp 283–297. ENSTA, Paris

Vermaas WFJ, Renger G and Dohnt G (1984) The reduction of the oxygen-evolving system in chloroplasts by thylakoid components. Biochim Biophys Acta 764: 194–202